24

Fuzzy Logic Based Interactive Multiple Model Fault Diagnosis for PEM Fuel Cell Systems

Yan Zhou[1,2], Dongli Wang[1], Jianxun Li[2],
Lingzhi Yi[1] and Huixian Huang[1]
[1]*College of Information Engineering, Xiangtan University, Xiangtan 411105,*
[2]*Department of Automation, Shanghai Jiao Tong University, Shanghai 200240,*
China

1. Introduction

The problem of fault detection and diagnosis (FDD) in dynamic systems has received considerable attention in last decades due to the growing complexity of modern engineering systems and ever increasing demand for fault tolerance, cost efficiency, and reliability (Willsky, 1976; Basseville, 1988). Existing FDD approaches can be roughly divided into two major categories including model-based and knowledge-based approaches (Venkatasubramanian et al., 2003a; Venkatasubramanian et al., 2003b). Model-based approaches make use of the quantitative analytical model of a physical system. Knowledge-based approaches do not need full analytical modeling and allow one to use qualitative models based on the available information and knowledge of a physical system. Whenever the mathematical models describing the system are available, analytical model-based methods are preferred because they are more amenable to performance analysis.

Generally, there are two steps in the procedure of model-based FDD. First, on the basis of the available observations and a mathematical model of the system, the state variable x and test statistics are required to be obtained. Then, based on the generated test statistics, it is required to decide on the potential occurrence of a fault. For linear and Gaussian systems, the Kalman filter (KF) is known to be optimal and employed for state estimation. The innovations from the KF are used as the test statistics, based on which hypothesis tests can be carried out for fault detection (Belcastro & Weinstein, 2002). In reality, however, the models representing the evolution of the system and the noise in observations typically exhibit complex nonlinearity and non-Gaussian distributions, thus precluding analytical solution. One popular strategy for estimating the state of such a system as a set of observations becomes available online is to use sequential Monte-Carlo (SMC) methods, also known as particle filters (PFs) (Doucet et al., 2001). These methods allow for a complete representation of the posterior probability distribution function (PDF) of the states by particles (Guo & Wang, 2004; Li & Kadirkamanathan, 2001).

The aforementioned FDD strategies are single-model-based. However, a single-model-based FDD approach is not adequate to handle complex failure scenarios. One way to treat this

problem is the interacting multiple model (IMM) filter (Zhang & Li, 1998). For the IMM approach, the single-model-based filters running in parallel interact each other in a highly cost-effective fashion and thus lead to significantly improved performance. The initial estimate at the beginning of each cycle for each filter is a mixture of all most recent estimates from the single-model-based filters. It is this mixing that enables the IMM to effectively take into account the history of the modes (and, therefore, to yield a more fast and accurate estimate for the changed system states) without the exponentially growing requirements in computation and storage as required by the optimal estimator. The probability of each mode is calculated, which indicates clearly the mode in effect and the mode transition at each time. This is directly useful for the detection and diagnosis of system failures. In view of these, there is a strong hope that it will be an effective approach to FDD and thus has been extensively studied during the last decade, see (Zhang & Jiang, 2001; Yen &Ho, 2003; Tudoroiu & Khorasani, 2005; Rapoport & Oshman, 2007), and reference therein.

A shortcoming of the IMM approach lies in that the mode declaration of the IMM filter may not reflect a true faulty situation because the model probability of the nominal model tends to become dominant especially when 1) the states and control inputs converge to the steady state at a nominal trim flight, or 2) a fault tolerant controller works well after the first failure. Besides, the IMM filter with the constant transition probability matrix has a problem diagnosing the second failure. To cope with the abovementioned problems, a new FDD technique is proposed using IMM filter and fuzzy logic for sensor and actuator failures. In this study, fuzzy logic is used to determinate the transition probability among the models not only to enhance the FDD performance after the first failure but also to diagnose the second one as fast and accurately as possible.

On the other hand, fuel cell technology offers high efficiency and low emissions, and holds great promise for future power generation systems. Recent developments in polymer electrolyte membrane (PEM) technology have dramatically increased the power density of fuel cells, and made them viable for vehicular and portable power applications, as well as for stationary power plants. A typical fuel cell power system consists of numerous interconnected components, as presented comprehensively in the books (Blomen & Mugerwa, 1993), (Larminie & Dicks, 2000), (Pukrushpan et al. 2004b), and more concisely in the survey paper (Carette et al. 2001) and (Kakac et al. 2007). Faults in the fuel cell systems can occur in sensors, actuators, and the other components of the system and may lead to failure of the whole system (Hernandez et al. 2010). They can be modeled by the abrupt changes of components of the system. Typical faults of main concern in the fuel cell systems are sensor or actuator failures, which will degrade or even disable the control performance. In the last a few years, a variety of FDD approaches have been developed for various failures (Riascos et al., 2007; Escobet et al., 2009; Gebregergis et al. 2010). However, only simple failure scenarios, such as failure in sensor or actuator, are concerned therein. Moreover, upon FDD problem for the PEM fuel cell systems, there is little result so far by IMM approach.

In this chapter, a self-contained framework to utilize IMM approach for FDD of PEM fuel cell systems is presented. As mentioned above, the constant transition probability matrix based IMM approach has problem in diagnosing the second failure, even though a fault tolerant controller works well after the first failure. Therefore, in our study, fuzzy logic is introduced to update the transition probability among multiple models, which makes the proposed FDD approach smooth and the possibility of false fault detection reduced. In

addition to the "total" (or "hard") actuator and/or sensor failures, "partial" (or "soft") faults are also considered. Compared with the existing results on FDD for fuel cell systems, more complex failure situations, including the total/partial senor and actuator failures, are considered. Simulation results considering both single and simultaneous sensor and/or actuator faults are given to illustrate the effectiveness of the proposed approach.

2. IMM for fault detection and diagnosis revisited

In this section, the details on generating the fault dynamics process using jump Markov linear hybrid dynamic models is first described. Then, the IMM estimation approach is developed for FDD.

2.1 Jump Markov hybrid systems

A stochastic hybrid system can be described as one with both continuous-valued base state and discrete-valued Structural/parametric uncertainty. A typical example of such a system is one subject to failures since fault modes are structurally different from each other and from the normal (healthy) mode. An effective and natural estimation approach for such a system is the one based on IMMs, in which a bank of filters running in parallel at every time with jumps in mode modeled as transition between the assumed models.

The IMM approach assumes that the state of the actual system at any time can be modeled accurately by the following jump Markov hybrid system:

$$x(k+1) = A(k, m(k+1))x(k) + B_u(k, m(k+1))u(k) + B_\omega(k, m(k+1))\omega(k, m(k+1)) \tag{1}$$

$$x(0) \in N(\hat{x}_0, P_0)$$

$$z(k) = C(k, m(k))x(k) + D_u(k, m(k))u(k) + D_\upsilon(k, m(k))\upsilon(k, m(k)) \tag{2}$$

with the system mode sequence assumed to be a first-order Markov chain with transition probabilities

$$P\{m_j(k+1) \mid m_i(k)\} = \pi_{ij}(k), \forall m_i, m_j \in S \tag{3}$$

and

$$\sum_j \pi_{ij}(k) = 1, 0 \le \pi_{ij}(k) \le 1, i = 1, ..., s \tag{4}$$

where $x(k)$ is the state vector, $z(k)$ is the mode-dependent measurement vector, and $u(k)$ is the control input vector; $\omega(k)$ and $\upsilon(k)$ are mutually independent discrete-time process and measurement noises with mean $\bar{\omega}(k)$ and $\bar{\upsilon}(k)$, and covariances $Q(k)$ and $R(k)$; $P\{\cdot\}$ is the probability operator; $m(k)$ is the discrete-value modal state (i.e., the index of the normal or fault mode in our FDD scenario) at time k, which denotes the mode in effect during the sampling period ending at t_k; π_{ij} is the transition probability from mode m_i to mode m_j; the event that m_j is in effect at time k is denoted as $m_j(k) := \{m(k) = m_j\}$. The mode set $S = \{m_1, m_2, ..., m_s\}$ is the set of all possible system modes.

The nonlinear system (1)-(2), known as a "jump linear system", can be used to model situations where the system behavior pattern undergoes sudden changes, such as system failures in this chapter and target maneuvering in (Li & Bar-Shalom, 1993). The FDD

problem in terms of the hybrid system may be stated as that of determining the current model state. That is, determining whether the normal or a faulty mode is in effect based on analyzing the sequence of noisy measurements.

How to design the set of models to represent the possible system modes is a key issue in the application of the IMM approach, which is problem dependent. As pointed in (Li, 1996), this design should be done such that the models (approximately) represent or cover all possible system modes at any time. This is the model set design problem, which will be discussed in the next subsection.

2.2 Model set design for IMM based FDD

In the IMM method, assume that a set of ***N*** models has been set up to approximate the hybrid system (1)-(2) by the following ***N*** pairs of equations:

$$x(k+1) = A_j(k)x(k) + B_{uj}(k)u(k) + B_{\omega j}(k)\omega(k) \tag{5}$$

$$z(k) = C_j(k)x(k) + D_{uj}(k)u(k) + D_{\upsilon j}(k)\upsilon(k) \tag{6}$$

where $N \le s$ and subscript j denotes quantities pertaining to model $m_j \in \mathcal{M}$ ($\mathcal{M}$ is the set of all designed system models to represent the possible system modes in S. System matrices A_j, B_{uj}, $B_{\omega j}$, C_j, D_{uj}, and $D_{\upsilon j}$ may be of different structures for different j.

The model set design (i.e., the design of fault type, magnitude, and duration) is critical for IMM based FDD. Design of a good set of models requires a priori knowledge of the possible faults of the system. As pointed out in (Li & Bar-Shalom, 1996; Li, 2000), caution must be exercised in designing a model set. For example, there should be enough separation between models so that they are "identifiable" by the IMM estimator. This separation should exhibit itself well in the measurement residuals, especially between the filters based on the matched models and those on the mismatched ones. Otherwise, the IMM fault estimator will not be very selective in terms of correct FDD because it is the measurement residuals that have dominant effects on the model probability computation which in turn affect the correctness of FDD and the accuracy of overall state estimates. On the other hand, if the separation is too large, numerical problems may occur due to ill conditions in the set of model likelihood functions. A total actuator failures may be modeled by annihilating the appropriate column(s) of the control input matrix B_u and D_u:

$$x(k+1) = A(k)x(k) + [B_u(k) + M_{Bj}]u(k) + B_\omega(k)\omega(k) \tag{7}$$

$$z(k) = C(k)x(k) + [D_u(k) + M_{dj}]u(k) + D_\upsilon(k)\upsilon(k) \tag{8}$$

That is, choose the matrix M_{Bj} with all zero elements except that the jth column is taken to be the negative of the jth column of B_u.

Alternatively, the jth actuator failure may be modeled by an additional process noise term $\varepsilon_j(k)$:

$$x(k+1) = A(k)x(k) + B_u(k)u(k) + B_\omega(k)\omega(k) + \varepsilon_j(k) \tag{9}$$

$$z(k) = C(k)x(k) + D_u(k)u(k) + D_\upsilon(k)\upsilon(k) + \varepsilon_j(k) \tag{10}$$

For total sensor failures, a similar idea can be followed. The failures can be modeled by annihilating the appropriate row(s) of the measurement matrix C described as

$$z(k) = [C(k) + L_j]x(k) + D_u(k)u(k) + D_\upsilon(k)\upsilon(k) \tag{11}$$

or by an additional sensor noise term $e_j(k)$

$$z(k) = C(k)x(k) + D_u(k)u(k) + D_\upsilon(k)\upsilon(k) + e_j(k) \tag{12}$$

Partial actuator (or sensor) failures are modeled by multiplying the appropriate column (or row) of B_u (or C) by a (scaling) factor of effectiveness. They can also be modeled by increasing the process noise covariance matrix Q or measurement noise covariance matrix R. Here we consider more complex failure situations, including total actuator and/or sensor failures, partial actuator and/or sensor failures, and simultaneous partial actuator and sensor failures. These situations require that the FDD algorithm be more responsive and robust. It is difficult for single-model-based approach to handle such complex failure scenarios.

2.3 Procedures of IMM approach to FDD

The following procedures should be performed in the application of the IMM estimation technique for fault detection and diagnosis: (i) filter reinitialization; (ii) model-conditional filtering; (iii) model probability updating; (iv) fault detection and diagnosis; (v) estimate fusion.

The detailed steps for the IMM algorithm are described next (Zhang & Li, 1998; Mihaylova & Semerdjiev, 1999; Johnstone & Krishnamurthy, 2001).

Step 1. Interaction and mixing of the estimates: filter reinitialization (interacting the estimates) obtained by mixing the estimates of all the filters from the previous time (this is accomplished under the assumption that a particular mode is in effect at the present time).

1. Compute the predicted model probability from instant k to k+1:

$$\mu_j(k+1 \mid k) = \sum_{i=1}^{N} \pi_{ij}\mu_i(k) \tag{13}$$

2. Compute the mixing probability:

$$\mu_{i|j}(k) = \pi_{ij}\mu_i(k) \big/ \mu_j(k+1 \mid k) \tag{14}$$

3. Compute the mixing estimates and covariance:

$$\hat{x}_j^0(k \mid k) = \sum_{i=1}^{N} \hat{x}_i(k \mid k)\mu_{i|j}(k) \tag{15}$$

$$P_j^0(k \mid k) = \sum_{i=1}^{N} \{P_i(k \mid k) + [\hat{x}_j^0(k \mid k) - \hat{x}_i(k \mid k)][\hat{x}_j^0(k \mid k) - \hat{x}_i(k \mid k)]^T\}\mu_{i|j}(k) \tag{16}$$

where the superscript 0 denotes the initial value for the next step.

Step 2. Model-conditional filtering
The filtering techniques such as (extended) Kalman filter, unscented Kalman filter, and particle filter can be applied for model-conditioning filtering. In this study, a linear Kalman filter is used as the individual filter of the IMM approach.
Step 2.1: Prediction step
1. Compute the predicted state and covariance from instant k to k+1:

$$\hat{x}_j(k+1|k) = A_j(k)\hat{x}_j^0(k|k) + B_{uj}(k)u(k) + B_{\omega j}(k)\bar{\omega}(k) \tag{17}$$

$$P_j(k+1|k) = A_j(k)P_j^0(k|k)A_j^T(k) + B_{\omega j}(k)Q_j(k)B_{\omega j}^T(k) \tag{18}$$

2. Compute the measurement residual and covariance:

$$r_j = z(k+1) - C_j(k+1)\hat{x}_j(k+1|k) - D_{uj}(k)u(k) - D_{\upsilon j}(k)\bar{\upsilon}(k) \tag{19}$$

$$S_j = C_j(k+1)P_j(k+1|k)C_j^T(k+1) + D_{\upsilon j}(k)R(k)D_{\upsilon j}^T(k) \tag{20}$$

3. Compute the filter gain:

$$K_j = P_j(k+1|k)C_j^T(k+1)S_j^{-1} \tag{21}$$

Step 2.2: Correction step
Update the estimated state and covariance matrix:

$$\hat{x}_j(k+1|k+1) = \hat{x}_j(k+1|k) + K_j r_j \tag{22}$$

$$P_j(k+1|k+1) = P_j(k+1|k) - K_j S_j K_j^T \tag{23}$$

Step 3. Updating the model probability
The model probability is an important parameter for the system fault detection and diagnosis. For this, a likelihood function should be defined in advance, and then the model probability be updated based on the likelihood function.
1. Compute the likelihood function:

$$L_j(k+1) = \frac{1}{\sqrt{2\pi|S_j|}}\exp\left[-\frac{1}{2}r_j^T S_j^{-1} r_j\right] \tag{24}$$

2. Update the model probability:

$$\mu_j(k+1) = \frac{\mu_j(k+1|k)L_j(k+1)}{\sum_{j=1}^{N}\mu_j(k+1|k)L_j(k+1)} \tag{25}$$

Step 4. Fault detection and diagnosis
1. Define the model probability vector $\vec{\mu}(k+1) = [\mu_1(k+1), \mu_2(k+1), ..., \mu_N(k+1)]$. The maximum value of the model probability vector for FDD can be obtained as

$$\mu_{\text{FDDmax}} = \max \vec{\mu}(k+1) \tag{26}$$

The index of the maximum value of the model probability vector component can be determined as

$$j = \text{find}(\mu_{\text{FDDmax}} == \vec{\mu}(k+1)) \tag{27}$$

2. Fault decision–FDD logic

The mode probabilities provide an indication of mode in effect at the current sampling period. Hence, it is natural to be used as an indicator of a failure. According to the information provided by the model probability, both fault detection and diagnosis can be achieved. The fault decision can be determined by

$$\mu_{\text{FDDmax}} \begin{cases} \geq \mu_T \Rightarrow H_j : \text{Delare fault corresponding to } j\text{th mode} \\ < \mu_T \Rightarrow H_1 : \text{No fault} \end{cases} \tag{28}$$

Or alternatively,

$$\frac{\mu_{\text{FDDmax}}}{\max\limits_{i \neq j} \vec{\mu}(k+1)} \begin{cases} \geq \mu_T^{'} \Rightarrow H_j : \text{Delare fault corresponding to } j\text{th mode} \\ < \mu_T^{'} \Rightarrow H_1 : \text{No fault} \end{cases} \tag{29}$$

Step 5. Estimate fusion and combination that yields the overall state estimate as the probabilistically weighted sum of the updated state estimates of all the filters. The probability of a mode in effect plays a key role in determining the weights associated with the fusion of state estimates and covariances. The estimates and covariance matrices can be obtained as:

$$\hat{x}(k+1 \mid k+1) = \sum_{j=1}^{N} \hat{x}_j(k+1 \mid k+1)\mu_j(k+1) \tag{30}$$

$$\begin{aligned} &P(k+1 \mid k+1) = \\ &= \sum_{j=1}^{N} [P_j(k \mid k) + (\hat{x}(k+1 \mid k+1) - \hat{x}_j(k+1 \mid k+1))(\hat{x}(k+1 \mid k+1) - \hat{x}_j(k+1 \mid k+1))^T]\mu_j(k+1) \end{aligned} \tag{31}$$

It will be seen from Section 4 that the transition probability plays an important role in the IMM approach to FDD. In this study, the transition probability is adapted online through the Takagi-Sugeno fuzzy logic (Takagi & Sugeno, 1985). The overall framework of the proposed fuzzy logic based IMM FDD algorithm is illustrated in Fig. 1.

It is worth noting that decision rule (28) or (29) provides not only fault detection but also the information of the type (sensor or actuator), location (which sensor or actuator), size (total failure or partial fault with the fault magnitude) and fault occurrence time, that is, simultaneous detection and diagnosis. For partial faults, the magnitude (size) can be determined by the probabilistically weighted sum of the fault magnitudes of the corresponding partial fault models. Another advantage of the IMM approach is that FDD is integrated with state estimation. The overall estimate provides the best state estimation of the system subject to failures. Furthermore, unlike other observer-based or Kalman filter

based approaches, there is no extra computation for the fault decision because the mode probabilities are necessary in the IMM algorithm. Furthermore, the overall estimate is generated by the probabilistically weighted sum of estimates from the single-model-based filters. Therefore, it is better and more robust than any single-model-based estimate. This state estimate does not depend upon the correctness of fault detection and in fact, the accurate state estimation can facilitate the correct FDD. The detection threshold μ_T is universal in the sense that it does not depend much on the particular problem at hand and a robust threshold can be determined easily. In other words, the FDD performance of the IMM approach varies little in most cases with respect to the choice of this threshold (Zhang & Li, 1998). On the other hand, the residual-based fault detection logic relies heavily on the threshold used, which is problem-relevant. Quite different detection thresholds have to be used for FDD problems of different systems and design of such a threshold is not trivial. Moreover, without comparing with the threshold, the value of the measurement residual itself does not provide directly meaningful detection and indication of the fault situations.

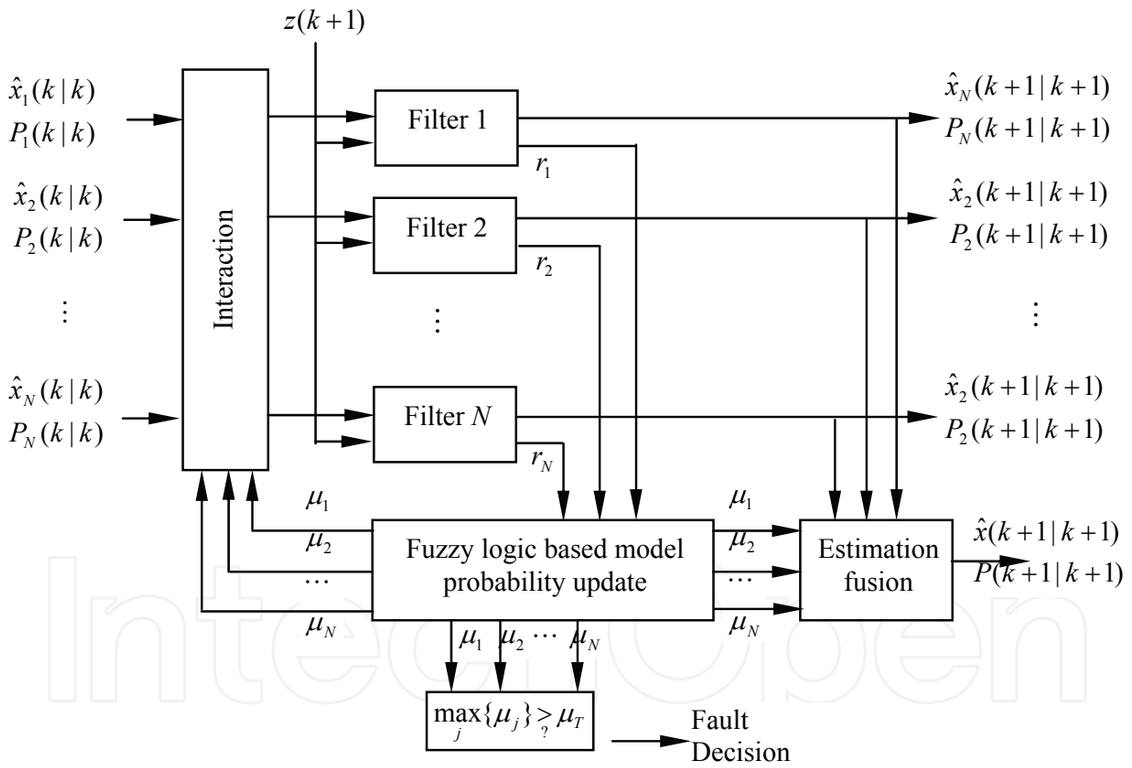

Fig. 1. Block diagram of the proposed fuzzy logic based IMM FDD approach

3. Update of transition probability by fuzzy logic

As aforementioned, the transition probability plays an important role in interacting and mixing the information of each individual filter. However, an assumption that the transition probability is constant over the total period of FDD can lead to some problems. Even if the fault tolerant control treats the first failure successfully, the unchanged transition probability

can mislead the FDD to intermittently declare a false failure alarm. This is because the fact that the normal mode before the first failure occurrence is not the normal mode any longer. The declared fault mode should be changed to a new normal mode after the first failure. On that account, the fuzzy-tuning algorithm of the transition probability is proposed in this study.

The transition probability from any particular failure mode to the normal mode is generally set larger than others in order to prevent a false fault diagnosis. However, it may have a bad influence on performing correct fault diagnosis because the model probability of the healthy mode tends to increase again as the current failed system converges to the steady state by the fault tolerant control law even after a fault occurs. This problem can be overcome by adjusting the transition probability after the fault occurrence. For example, if the model probability of a certain failure mode remains larger than that of any other mode for an assigned time, the transition probability related to the corresponding failure mode should be increased. On the other hand, the transition probability related to the previous mode should be decreased to reflect the fact that the failed mode selected by the fault decision algorithm becomes currently dominant. In this work, the fuzzy-tuning algorithm is adopted to adjust the transition probabilities effectively.

Now introduce a determination variable C_i which decides whether or not the transition probabilities should be adjusted. First, the initial value of each mode's determination variable is set to zero. The increment of the determination variable can be obtained through the fuzzy logic with inputs composed of the model probabilities at every step. If the determination variable C_i of a certain mode exceeds a predefined threshold value C_T, then the transition probabilities are adjusted, and the determination value of each mode is initialized. The overall process is illustrated in Fig. 2.

3.1 Fuzzy input

A fuzzy input for adjusting transition probabilities includes the model probabilities from the IMM filter. At each sampling time, the model probabilities of every individual filter are transmitted to the fuzzy system. In this work, the membership function is designed as in Fig. 3 for the fuzzy input variables "small," "medium," and "big" representing the relative size of the model probability.

3.2 Fuzzy rule

The T-S fuzzy model is used as the inference logic in this work. The T-S fuzzy rule can be represented as

$$\text{If } \chi \text{ is } A \text{ and } \xi \text{ is } B \text{ then } Z = f(\chi, \xi) \tag{32}$$

where A and B are fuzzy sets, and $Z = f(\chi, \xi)$ is a non-fuzzy function. The fuzzy rule of adjusting transition probabilities is defined using the T-S model as follows

$$\begin{aligned} &\text{If } \mu_j \text{ is small, then } \Delta C_j^s = 0 \\ &\text{If } \mu_j \text{ is medium, then } \Delta C_j^m = 0.5 \\ &\text{If } \mu_j \text{ is big, then } \Delta C_j^b = 1 \end{aligned} \tag{33}$$

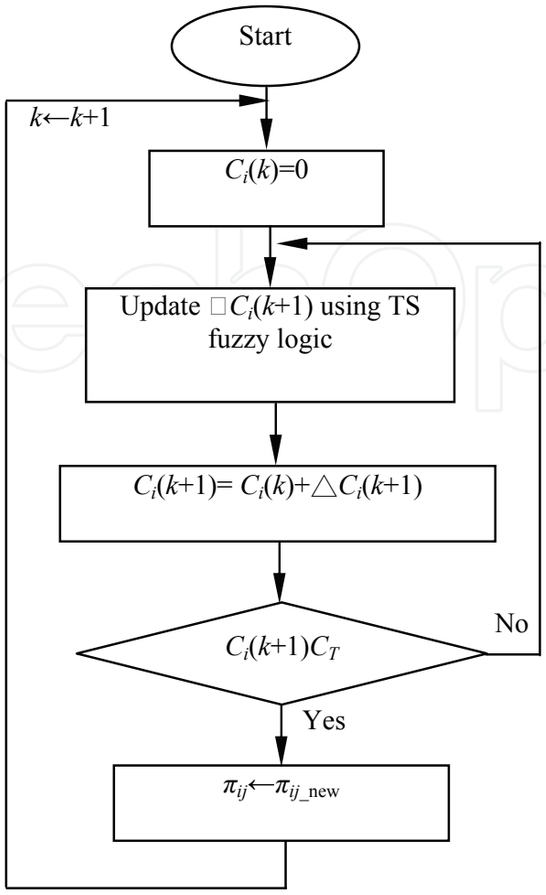

Fig. 2. Flowchart of T-S fuzzy logic for adaptive model probability update

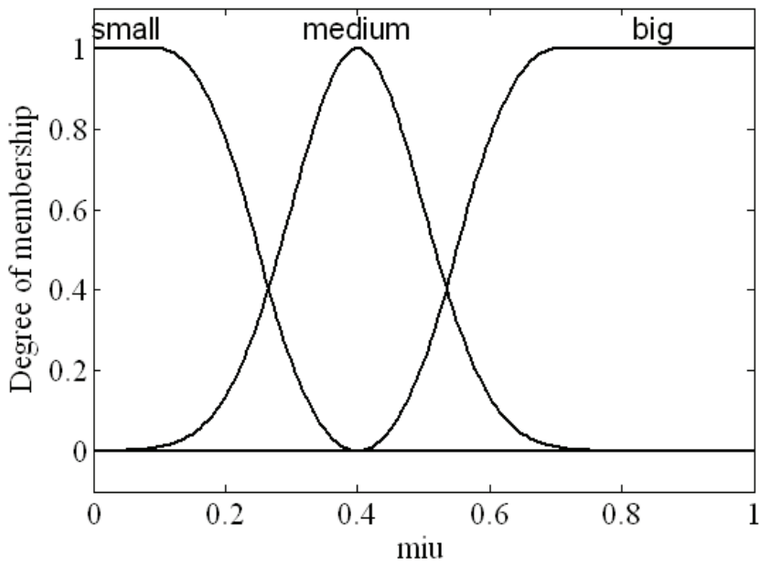

Fig. 3. Fuzzy membership function

3.3 Fuzzy output

The output of the fuzzy system using the T-S model can be obtained by the weighted average using a membership degree in a particular fuzzy set as follows:

$$\Delta C_j(k) = \frac{w_j^s \Delta C_j^s + w_j^m \Delta C_j^m + w_j^b \Delta C_j^b}{w_j^s + w_j^m + w_j^b} \tag{34}$$

where w_j^s, w_j^m, and w_j^b is the membership degree in the jth mode for group small, medium, and big, respectively. During the monitoring process, the determination variable of the jth mode is accumulated as

$$\Delta C_j(k+1) = C_j(k) + \Delta C_j(k+1) \tag{35}$$

The designed fuzzy output surface of the T-S fuzzy interference system is shown in Fig. 4.

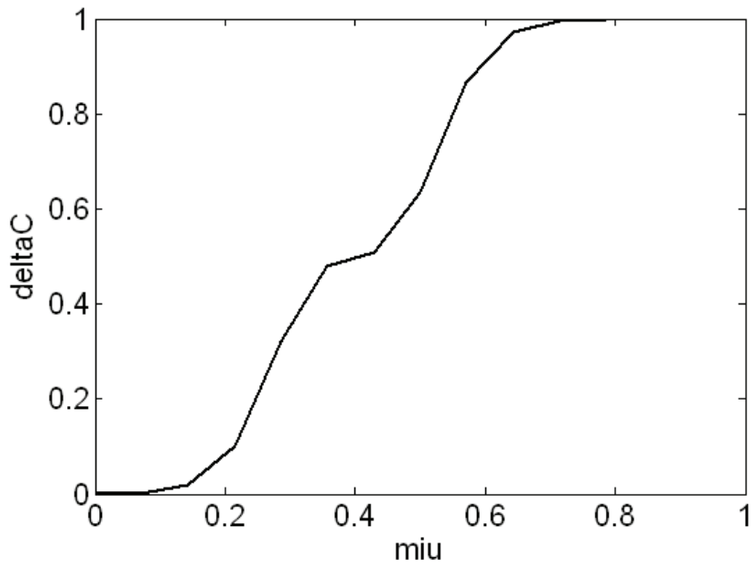

Fig. 4. Output surface of the fuzzy interference system

Once the determination variable of a certain fault mode exceeds the threshold value C_T, then all the elements of the transition probability matrix from the other modes to the corresponding fault mode are increased.

3.4 Transition probability design

The diagonal elements of the transition probability matrix can be designed as follows (Zhang & Li, 1998).

$$\pi_{jj} = \max\left\{ l_j, 1 - \frac{T}{\tau_j} \right\} \tag{36}$$

where T, τ_j, and l_j are the sampling time, the expected sojourn time, and the predefined threshold of the transition probability, respectively. For example, the "normal-to-normal"

transition probability, π_{11}, can be obtained by $\pi_{11} = 1 - T/\tau_1$ (here τ_1 denotes the mean time between failures) since T is much smaller than τ_1 in practice. The transition probability from the normal mode to a fault mode sums up to $1 - \pi_{11}$. To which particular fault mode it jumps depends on the relative likelihood of the occurrence of the fault mode. While in reality mean sojourn time of total failures is the down time of the system, which is usually large and problem-dependent, to incorporate various fault modes into one sequence for a convenient comparison of different FDD approaches, the sojourn time of the total failures is assumed to be the same as that of the partial faults in this work.

"Fault-to-fault'' transitions are normally disallowed except in the case where there is sufficient prior knowledge to believe that partial faults can occur one after another. Hence, by using (36), the elements of the transition probability related to the current model can be defined by

$$p_n = 1 - \frac{T}{\tau_n}, \quad \tilde{p}_n = \frac{1 - p_n}{N - 1} \tag{37}$$

$$p_f = 1 - \frac{T}{\tau_f}, \quad \tilde{p}_f = 1 - p_f \tag{38}$$

where p_n and p_f are the diagonal elements of the normal and failure mode, respectively, and $\tilde{p}_n$ and $\tilde{p}_f$ are off-diagonal elements to satisfy the constraint that all the row sum of the transition probability matrix should be equal to one. In addition, N is the total number of the assumed models, and τ_n and τ_f are the expected sojourn times of the normal and failure mode, respectively.

After a failure declaration by the fuzzy decision logic, the transition probability from the other modes to the corresponding failure model (say the mth mode) should be increased, whereas the transition probabilities related to the nonfailed model should be relatively decreased. For this purpose, the transition probability matrix of each mode is set as follows.

$$\pi_{ij} = \begin{cases} p_n, & i = j = m \\ p_f, & i = j \neq m \\ \tilde{p}_n, & i = j \text{ and } j \neq m \\ p_f, & i \neq m \text{ and } j = m \\ 0, & \text{otherwise} \end{cases} \tag{39}$$

4. PEM fuel cell description and modeling

The fuel cell system studied in this work is shown in Fig. 5. It is assumed that the stack temperature is constant. This assumption is justified because the stack temperature changes relatively slowly, compared with the ~100 ms transient dynamics included in the model to be developed. Additionally, it is also assumed that the temperature and humidity of the inlet reactant flows are perfectly controlled, e.g., by well designed humidity and cooling subsystems. It is further assume that the cathode and anode volumes of the multiple fuel cells are lumped as a single stack cathode and anode volumes. The anode supply and return manifold volumes are small, which allows us to lump these volumes to one ''anode''

volume. We denote all the variables associated with the lumped anode volume with a subscript (an). The cathode supply manifold (sm) lumps all the volumes associated with pipes and connection between the compressor and the stack cathode (ca) flow field.The cathode return manifold (rm) represents the lumped volume of pipes downstream of the stack cathode. In this study, an expander is not included; however, we will consider this part in future models for FDD. It is assumed that the properties of the flow exiting a volume are the same as those of the gas inside the volume. Subscripts (cp) and (cm) denote variables associated with the compressor and compressor motor, respectively.

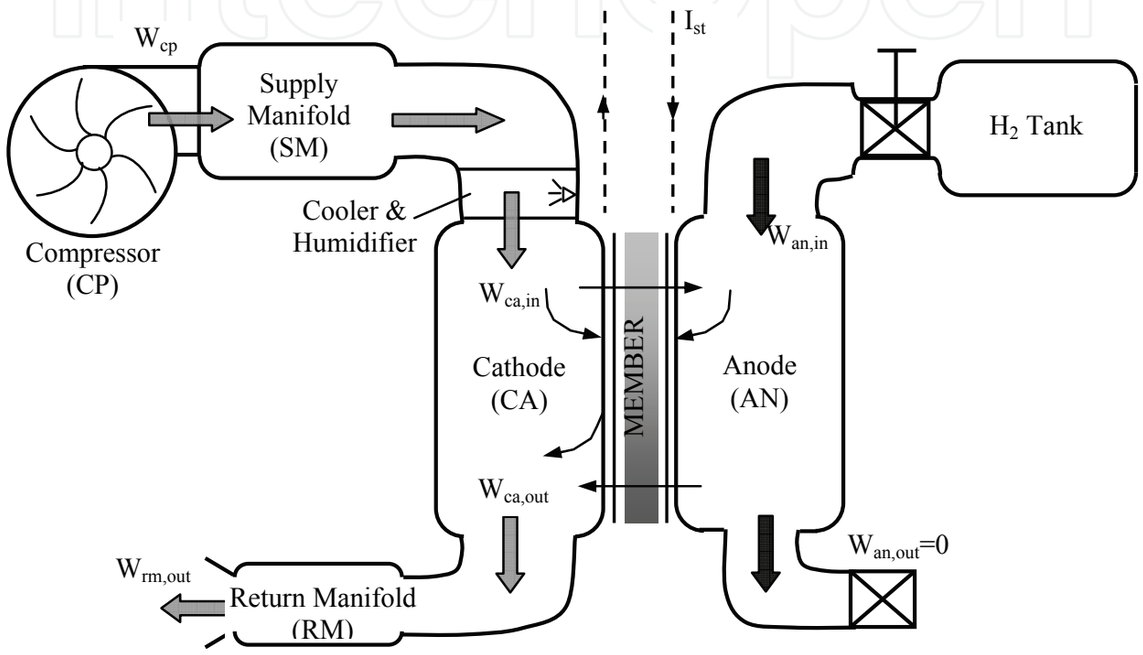

Fig. 5. Simplified fuel cell reactant supply system

The rotational dynamics and a flow map are used to model the compressor. The law of conservation of mass is used to track the gas species in each volume. The principle of mass conservation is applied to calculate the properties of the combined gas in the supply and return manifolds. The law of conservation of energy is applied to the air in the supply manifold to account for the effect of temperature variations. Under the assumptions of a perfect humidifier and air cooler, and the use of proportional control of the hydrogen valve, the only inputs to the model are the stack current, I_{st}, and the compressor motor voltage, v_{cm}. The parameters used in the model are given in Table 1 (Pukrushpan et al., 2004a). The model is developed primarily based on physics. However, several phenomena are described in empirical equations. The models for the fuel cell stack, compressor, manifolds, air cooler and humidifier are presented in state-space model as specified by (40)-(41) with the relating matrices given in Table 1.

$$\dot{x} = A_c x + B_{uc} u + b_{\omega c} \omega \tag{40}$$

$$z = C_c x + D_{uc} u + D_{\omega c} \omega \tag{41}$$

where $u=[v_{cm}, I_{st}]^T$, and $z=[W_{cp}, p_{sm}, v_{st}]^T$, the stochastic noise or disturbance ω models the uncertainties caused by the linearization and measurement noises, etc. Note that the nominal operating point is chosen to be P_{net}=40 kW and λ_{O2} =2, which correspond to nominal inputs of I_{st}=191 Amp and v_{cm}=164 Volt. The state vector $x=[m_{O_2}, m_{H_2}, m_{N_2}, \omega_{cp}, p_{sm}, m_{sm}, m_{O_2}, m_{w,an}, p_{rm}]^T$. In more details, the fuel cell system model developed above contains eight states. The compressor has one state: rotor speed. The supply manifold has two states: air mass and air pressure. The return manifold has one state: air pressure. The stack has four states: O_2, and N_2 masses in the cathode, and H_2 and vapor masses in the anode. These states then determine the voltage output of the stack.

Symbol	Variable	Value
$r_{m,dry}$	Membrane dry density	0.002 kg/cm^3
$M_{m,dry}$	Membrane dry equivalent weight	1.1 kg/mol
t_m	Membrane thickness	0.01275 cm
n	Number of cells in stack	381
A_{fc}	Fuel cell active area	280 cm^2
d_c	Compressor diameter	0.2286 m
J_{cp}	Compressor and motor inertia	531025 kg.m^2
V_{an}	Anode volume	0.005 m^3
V_{ca}	Cathode volume	0.01 m^3
V_{sm}	Supply manifold volume	0.02 m^3
V_{rm}	Return manifold volume	0.005 m^3
$C_{D,rm}$	Return manifold throttle discharge coefficient	0.0124
$A_{T,rm}$	Return manifold throttle area	0.002 m^2
$k_{sm,out}$	Supply manifold outlet orifice constant	0.362931025 kg/(s.Pa)
$k_{ca,out}$	Cathode outlet orifice constant	0.217731025 kg(s.Pa)
k_v	Motor electric constant	0.0153 V/(rad/s)
k_t	Motor torque constant	0.0153 N-m/A
R_{cm}	Compressor Motor circuit resistance	0.816 V
h_{cm}	Compressor Motor efficiency	98%

Table 1. Model parameters for vehicle-size fuel cell system

Three measurements are investigated: compressor air flow rate, $z_1=W_{cp}$, supply manifold pressure, $z_2=p_{sm}$, and fuel cell stack voltage, $z_3=V_{st}$. These signals are usually available because they are easy to measure and are useful for other purposes. For example, the compressor flow rate is typically measured for the internal feedback of the compressor. The stack voltage is monitored for diagnostics and fault detection purposes. Besides, the units of states and outputs are selected so that all variables have comparable magnitudes, and are as follows: mass in grams, pressure in bar, rotational speed in kRPM, mass flow rate in g/sec, power in kW, voltage in V, and current in A.

In this study, the simultaneous actuator and sensor faults are considered. The fuel cell systems of interest considered here have two actuators and three sensors. Therefore, there are potentially only six modes, with the first mode being designated as the normal mode as (40)-(41) and the other five modes designated as the faulty modes associated with each of the faulty actuators or sensors.

$$A_c = \begin{bmatrix} -6.30908 & 0 & -10.9544 & 0 & 83.74458 & 0 & 0 & 24.05866 \\ 0 & -161.083 & 0 & 0 & 51.52923 & 0 & -18.0261 & 0 \\ -18.7858 & 0 & -46.3136 & 0 & 275.6592 & 0 & 0 & 158.3741 \\ 0 & 0 & 0 & -17.3506 & 193.9373 & 0 & 0 & 0 \\ 1.299576 & 0 & 2.969317 & 0.3977 & -38.7024 & 0.105748 & 0 & 0 \\ 16.64244 & 0 & 38.02522 & 5.066579 & -479.384 & 0 & 0 & 0 \\ 0 & -450.386 & 0 & 0 & 142.2084 & 0 & -80.9472 & 0 \\ 2.02257 & 0 & 4.621237 & 0 & 0 & 0 & 0 & -51.2108 \end{bmatrix}$$

$$C_c = \begin{bmatrix} 0 & 0 & 0 & 5.066579 & -116.446 & 0 & 0 & 0 \\ 0 & 0 & 0 & 0 & 1 & 0 & 0 & 0 \\ 12.96989 & 10.32532 & -0.56926 & 0 & 0 & 0 & 0 & 0 \end{bmatrix}$$

$$B_{uc} = \begin{bmatrix} 0 & 0 & 0 & 3.94668 & 0 & 0 & 0 & 0 \\ -0.03159 & -0.00398 & 0 & 0 & 0 & 0 & -0.05242 & 0 \end{bmatrix}^T, \quad D_{uc} = \begin{bmatrix} 0 & 0 \\ 0 & 0 \\ 0 & -0.29656 \end{bmatrix}$$

Table 2. Parameters for the linear fuel cell model in (40)-(41)

$$A_1 = \begin{bmatrix} 0.1779 & 0 & -0.0333 & 0.0047 & -0.1284 & 0.0245 & 0 & -0.02 \\ 0.0012 & 0 & 0.0004 & 0.0002 & -0.0169 & 0.0019 & 0 & 0.002 \\ -0.0401 & 0 & 0.0263 & 0.0038 & -0.3963 & 0.0415 & 0 & 0.0663 \\ 0.0444 & 0 & 0.0177 & 0.0079 & -0.5741 & 0.0676 & 0 & 0.0806 \\ 0.0036 & 0 & 0.0012 & 0.0006 & -0.0517 & 0.0057 & 0 & 0.0059 \\ 0.0408 & 0 & 0.01 & 0.0053 & -3.9786 & 0.3265 & 0 & 0.0543 \\ -0.0004 & 0 & -0.0003 & -0.0001 & 0.0031 & -0.0005 & 0 & -0.0011 \\ 0.0035 & 0 & 0.0011 & 0.0006 & -0.0408 & 0.0048 & 0 & 0.0055 \end{bmatrix}$$

$$B_{u1} = \begin{bmatrix} 0.0451 & -0.0145 \\ 0.004 & 0 \\ 0.0878 & 0.0034 \\ 0.3634 & -0.0028 \\ 0.0123 & -0.0003 \\ 0.1474 & -0.0032 \\ -0.0007 & 0.0013 \\ 0.0097 & -0.0003 \end{bmatrix}$$

$$C_1 = \begin{bmatrix} 0 & 0 & 0 & 5.0666 & -116.446 & 0 & 0 & 0 \\ 0 & 0 & 0 & 0 & 1 & 0 & 0 & 0 \\ 12.9699 & 10.3253 & -0.5693 & 0 & 0 & 0 & 0 & 0 \end{bmatrix}$$

$$D_{u1} = \begin{bmatrix} 0 & 0 \\ 0 & 0 \\ 0 & -0.2966 \end{bmatrix}$$

Table 3. Parameters for the discretized model

Actuator (or control surface) failures were modeled by multiplying the respective column of B_{u1} and D_{u1}, by a factor between zero and one, where zero corresponds to a total (or complete) actuator failure or missing control surface and one to an unimpaired (normal) actuator/control surface. Likewise for sensor failures, where the role of B_{u1} and D_{u1} is

replaced with C_1. It was assumed that the damage does not affect the fuel cell system dynamic matrix A_1, implying that the dynamics of the system are not changed.
Let sampling period $T = 1$ s. Discretization of (40)-(41) yields the matrices for normal mode $A_1 = e^{A_c T}$, $B_{u1} = (\int_0^T e^{A_c \tau} d\tau) B_c$, $B_{\omega 1} = (\int_0^T e^{A_c \tau} d\tau) B_{\omega c}$, $C_1 = C_c$, $D_{u1}, = D_{u1}$, $D_{\upsilon 1}, = D_{\upsilon 1}$, which are specified in Table 3.
The fault modes in this work are more general and complex than those considered before, including total single sensor or actuator failures, partial single sensor or actuator failures, total and partial single sensor and/or actuator failures, and simultaneous sensor and actuator failures.

5. Results and discussion

Scenario 1: Single total/partial actuator faulty mode

First, in order to compare the performance between the conventional IMM and the proposed fuzzy logic based IMM approach, consider the simplest situation in which only a single total (or partial) sensor or actuator is running failure. Specifically, only partial failure for the actuator according to the second control input, i.e. stack current, I_{st}, is considered. The failure occurs after the 50th sampling period with failure amplitude of 50%. Two models consisting the normal mode and second actuator failure with amplitude of 50% are used for the IMM filter. The fault decision criterion in (29) is used with the threshold $\mu_T^{'} = 2.5$. The transition matrix for the conventional IMM and the initial for the proposed approach are set as follows

$$\Pi = \begin{bmatrix} 0.99 & 0.01 \\ 0.1 & 0.9 \end{bmatrix}$$

The results of the FDD based on our proposed approach are compared with that of the conventional IMM filter. Fig. 6 (a) and (b) represent the model probabilities of the 2 models and the mode index according to (29) for the conventional IMM, respectively. From Fig. 6, it is obvious that the model probability related to the failure model does not keep a dominant value for the conventional IMM approach. On that account, momentary false failure mode is declared after the failure although the approach works well before the first failure occurs,

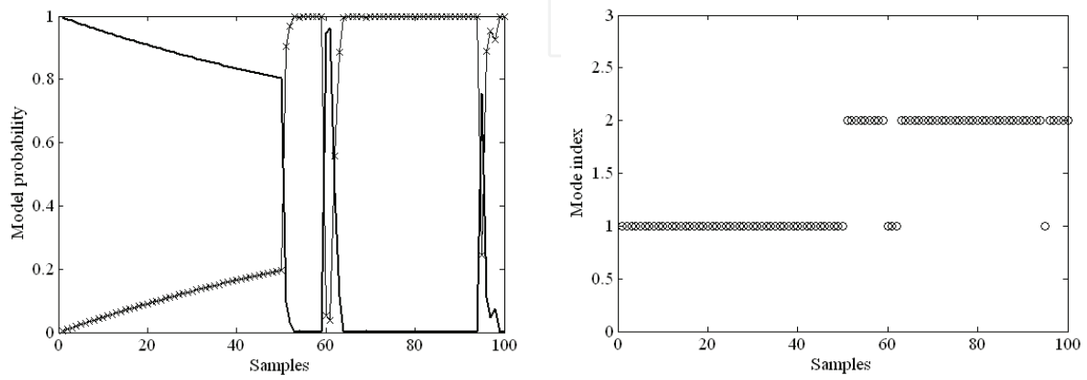

Fig. 6. The model probabilities and the mode index for the conventional IMM approach

just as shown in Fig. 6 (b). The performance of the proposed fuzzy logic based IMM approach is stable to hold a higher model probability than that of the conventional filter (cf. Fig. 7 (a)-(b)). This concludes that the improved IMM approach has better performance and, more importantly, reliability that the conventional IMM filter.

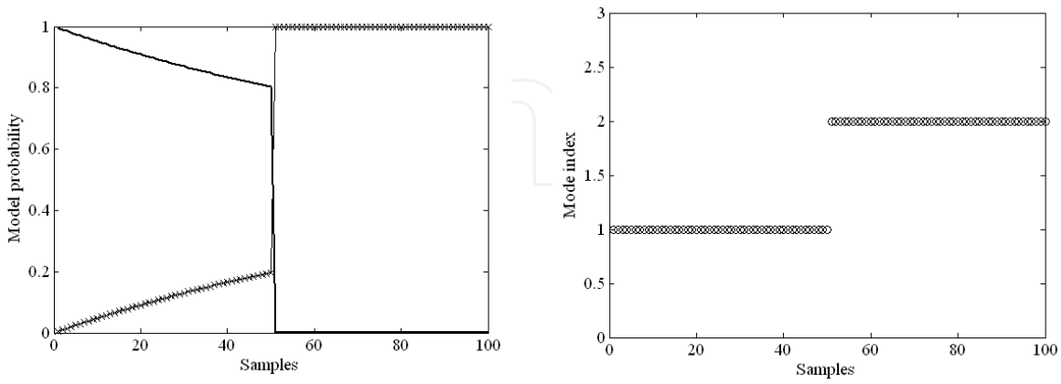

Fig. 7. The model probabilities and the mode index for the proposed fuzzy logic based IMM approach

Scenario 2: Single total/partial sensor/actuator faulty mode sequence

Consider the situation in which only a single total (or partial) sensor or actuator failure is possible. Then there are a total of 4 possible model (one normal plus 3 failure models) for sensor failure and 3 possible models (one normal plus 2 failure models) for actuator failures. Similarly, there are 4 partial sensor failure models and 3 partial actuator failures models. Due to the space limitation, only the simulation results for the sensor failure case are presented herein. Let the pairs (z_1, u_n), (z_2, u_{s1}), (z_3, u_{s2}), (z_4, u_{s3}) designate the measurements and corresponding causes associated with the normal/fault-free mode, and sensor fault for the first to the third sensor, respectively. Furthermore, let the pair (z_5, u_{s3p}) denote the measurement and corresponding causes associated with the partial fault for the third sensor. Consider the sequence of events designated by z=[z_1, z_2, z_1, z_3, z_1, z_4, z_1, z_5, z_1] and u=[u_n, u_{s1}, u_n, u_{s2}, u_n, u_{s3}, u_n, u_{s3p}, u_n], where the first, second, third total sensor failures, and the partial third sensor failure occur at the beginning of the time horizon windows [31, 50], [81, 110], [141, 180], and [211, 250], respectively. Note that z_1 corresponds to the normal mode. The faults persist for the duration of 20, 30, 40, and 40 samples, respectively.

Let the initial model probability for both the conventional IMM and the fuzzy logic based IMM approach $\mu(0) =$ [0.2, 0.2, 0.2, 0.2, 0.2]^T. The transition matrix for the conventional IMM and the initial one for the proposed approach are set as

$$\Pi = \begin{bmatrix} 0.96 & 0.01 & 0.01 & 0.01 & 0.01 \\ 0.1 & 0.9 & 0 & 0 & 0 \\ 0.1 & 0 & 0.9 & 0 & 0 \\ 0.1 & 0 & 0 & 0.9 & 0 \\ 0.1 & 0 & 0 & 0 & 0.9 \end{bmatrix}$$

The mode indexes as a function of sampling period for the conventional IMM and the fuzzy logic based IMM approach are compared in Fig. 8.

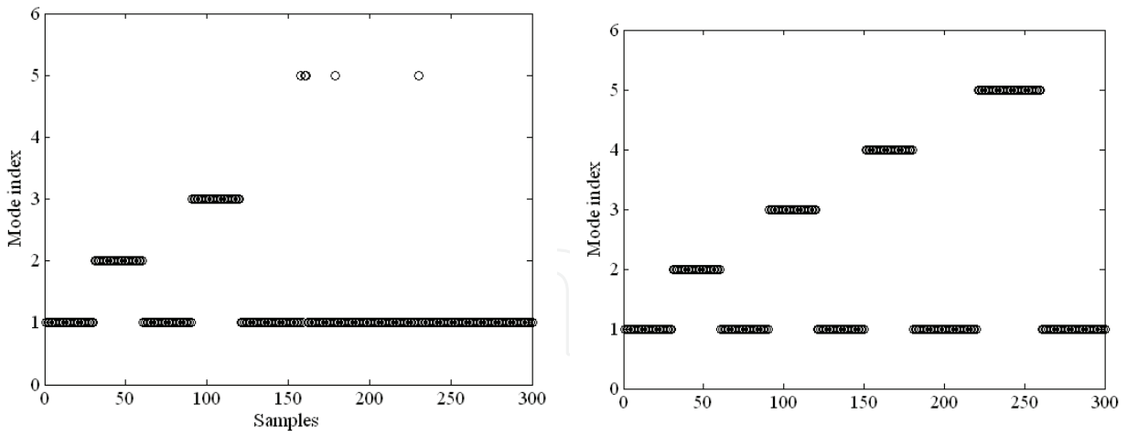

Fig. 8. The mode index in the 2nd scenario for (a) the conventional IMM; and (b) the fuzzy logic based IMM

Scenario 3: Simultaneous faulty modes sequence

Let the pairs (z_1, u_n), (z_2, u_{s1}), (z_3, u_{s2}), (z_4, u_{s3}), (z_5, u_{a1}), (z_6, u_{a2}) stand for the measurements and corresponding causes associated with the normal mode, sensor fault for the first to the third sensor, and the actuator fault for the first and second actuator, respectively. Furthermore, let (z_7, u_{a1s2}), (z_8, u_{a2s2}), (z_9, u_{a1a2}), (z_{10}, u_{a1s3}), (z_{11}, u_{a2s3}), (z_{12}, u_{s2s3}) designate the measurements and the inputs due to the presence of simultaneous double faulty modes caused by different combination of sensors and actuators, respectively. For simplicity and clarity, only sensor and actuator partial failures are considered herein.

The initial model probabilities are $\mu(0) = 1/N$, where N = 12 represents the number of modes; the threshold model probability $\mu_T' = 2.5$; and the initial one for the proposed approach are set as

$$\Pi = \begin{bmatrix} a & b & b & b & b & b & b & b & b & b & b & b \\ d & c & 0 & 0 & 0 & 0 & 0 & 0 & 0 & 0 & 0 & 0 \\ d & 0 & c & 0 & 0 & 0 & 0 & 0 & 0 & 0 & 0 & 0 \\ d & 0 & 0 & c & 0 & 0 & 0 & 0 & 0 & 0 & 0 & 0 \\ d & 0 & 0 & 0 & c & 0 & 0 & 0 & 0 & 0 & 0 & 0 \\ d & 0 & 0 & 0 & 0 & c & 0 & 0 & 0 & 0 & 0 & 0 \\ d & 0 & 0 & 0 & 0 & 0 & c & 0 & 0 & 0 & 0 & 0 \\ d & 0 & 0 & 0 & 0 & 0 & 0 & c & 0 & 0 & 0 & 0 \\ d & 0 & 0 & 0 & 0 & 0 & 0 & 0 & c & 0 & 0 & 0 \\ d & 0 & 0 & 0 & 0 & 0 & 0 & 0 & 0 & c & 0 & 0 \\ d & 0 & 0 & 0 & 0 & 0 & 0 & 0 & 0 & 0 & c & 0 \\ d & 0 & 0 & 0 & 0 & 0 & 0 & 0 & 0 & 0 & 0 & c \end{bmatrix}$$

where $a = 19/20$, $b = 1/220$, $c = 9/10$, and $d = 1/10$. Two faulty sequences of events are considered. The first sequence is 1-2-3-4-6-12, for which the events occur at the beginning of the 1st, 51st, 101st, 141st, 201st, 251st sampling point, respectively. The second sequence is 1-3-

5-7-8-9-10-11-12, for which the events occur at the beginning of the 1st, 41st, 71st, 111st, 141st, 181st, 221st, 251st, 281st sampling point, respectively. Note that z_1 corresponds to the normal mode. Then, for the first case the faults persist for the duration of 40, 40, 60, 50, and 50 samples within each window. For the second case the faults persist for 30, 40, 30, 40, 40, 30, 30, and 20 samples, respectively. For space reason, only the performance and capabilities of the proposed approach are shown. The results for the two cases are shown in Fig. 9 and Fig. 10, respectively. A quick view on the results, we may find that there is generally only one step of delay in detecting the presence of the faults. However, a more insight on both figures may reveal that at the beginning of the mode 4, it always turns out to be declared as mode 10, while taking mode 8 for mode 12, and vice versa. This may be attributed to the similarity between the mode 4 and 10, 8 and 12. However, the results settled down quickly, only 5-6 samples on average.

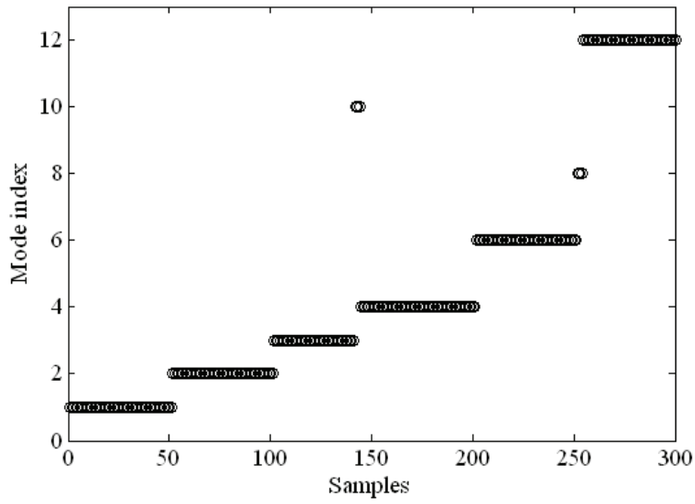

Fig. 9. The mode index in the 3rd scenario of sequence 1-2-3-4-6-12

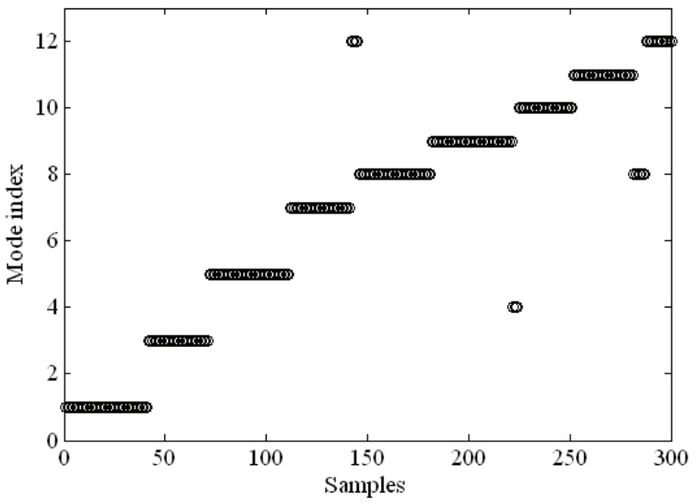

Fig. 10. The mode index in the 3rd scenario of sequence 1-3-5-7-8-9-10-11-12

6. Conclusion and future work

A self-contained framework to utilize IMM approach for fault detection and diagnosis for PEM fuel cell systems has been presented in this study. To overcome the shortcoming of the conventional IMM approach with constant transition matrix, a Takagi-Sugeno fuzzy model has been introduced to update the transition probability among multiple models, which makes the proposed FDD approach smooth and the possibility of false fault detection reduced. Comparing with the existing results on FDD for fuel cell systems , "partial" (or "soft") faults in addition to the "total" (or "hard") actuator and/or sensor failures have also been considered in this work. Simulation results for three different scenarios considering both single and simultaneous sensor and/or actuator faults have been given to illustrate the effectiveness of the proposed approach.

The scenarios considered correspond to representative symptoms in a PEM fuel cell system, and therefore the set of the considered models can't possibly cover all fault situations that may occur. Note that in case the fuel cell system undergoes a fault that it has not seen before, there is a possibility that the system might become unstable as a result of the IMM algorithm decision. It is indeed very difficult to formally and analytically characterize this, but based on our extensive simulation results presented, all the faulty can be detected precisely and timely.

It is worth mentioning that the main objective of this work was to develop and present simulation results for the applicability and the effectiveness of the fuzzy logic based IMM approach for fault diagnosis of a PEM fuel cell system. The proposed approach can be readily extended to IMM-based fault-tolerant control and provides extremely useful information for system compensation or fault-tolerant control subsequent to the detection of a failure. This work is under investigation and will be reported in the near future.

7. Acknowledgements

The work was supported by the National Natural Science Foundation of China (Under Grant 60874104, 60935001), and the Ph.D Scientific Research Foundation from Xiangtan University (Under Grant 10QDZ22).

8. References

Basseville, M. (1988). Detecting changes in signals and systems–A survey. *Automatica*, vol. 24, no. 3, pp. 309—326

Belcastro, C.M.; & Weinstein, B. (2002). Distributed detection with data fusion for malfunction detection and isolation in fault tolerant flight control computers. *Proceedings of the American Control Conference*, Anchorage, AK, May 2002

Blomen, L.; & Mugerwa, M. (1993). *Fuel Cell Systems*. New York: Plenum Press

Carette, L.; Friedrich, K.; & Stimming, U. (2001). Fuel cells – fundamentals and applications. *Fuel Cells Journal*, vol. 1, no. 1, pp. 5–39

Doucet, A.; de Freitas, N.; & Gordon, N. (2001) *Sequential Monte Carlo Methods in Practice*. New York: Springer-Verlag

Escobet, T.; Feroldi, D.; de Lira, S. et al. (2009). Model-based fault diagnosis in PEM fuel cell systems. *Journal of Power Sources*, vol. 192, no. 6, pp. 216-223

Gebregergis, A.; Pillay, P.; & Rengaswamy, R. (2010). PEMFC Fault Diagnosis, Modeling, and Mitigation, *IEEE Transactions on Industry Applications*, vol. 46, no. 1, pp. 295-303

Guo, D.; & Wang, X. (2004). Dynamic sensor collaboration via sequential Monte Carlo. *IEEE Journal on Selected Areas in Communications*, vol. 22, no. 6, pp. 1037—1047

Hernandez, A.; Hissel, D.; & Outbib, R. (2010). Modeling and Fault Diagnosis of a Polymer Electrolyte Fuel Cell Using Electrical Equivalent Analysis, *IEEE Transactions on Energy Conversion*, vol. 25, no. 1, pp. 148-160

Johnstone, A.L.; & Krishnamurthy, V. (2001). An improvement to the interacting multiple model algorithm. *IEEE Transactions on Signal Processing*, vol. 49, no. 12, pp. 2909—2923

Kakac, S.; Pramuanjaroenkijb, A.; & Zhou, X.Y. (2007). A review of numerical modeling of solid oxide fuel cells. *International Journal of Hydrogen Energy*, vol. 32, no. 7, pp. 761-786

Larminie, J.; & Dicks, A. (2000). *Fuel Cell Systems Explained*. Chicester: John Wiley & Sons, Inc.

Li, P.; & Kadirkamanathan, V. (2001). Particle filtering based likelihood ratio approach to fault diagnosis in nonlinear stochastic systems. *IEEE Transactions on Systems, Man, and Cybernetics, Part C*, vol. 31, no. 3, pp. 337—343

Li, X.R. (1996). Hybrid estimation techniques. In Leondes, C.T. (Ed.), *Control and Dynamic Systems,* vol. 76. New York: Academic Press, pp. 213-287

Li, X.R. (2000). Multiple-model estimation with variable structure-part II: model-set adaptation. *IEEE Transactions on Automatic Control*, vol. 45, no. 11, pp. 2047-2060

Li, X.R.; & Bar-Shalom, Y. (1993). Design of an interacting multiple model algorithm for air traffic control tracking. *IEEE Transactions on Control System Technology,* vol. 1, no. 3, pp. 186-194

Li, X.R., & Bar-Shalom, Y. (1996). Multiple model estimation with variable structure. *IEEE Transactions on Automatic Control*, vol. 41, no. 4, pp. 478-493

Mihaylova, L.; & Semerdjiev, E. (1999). Interacting multiple model algorithm for maneuvering ship tracking based on new ship models. *Information and Security*, vol. 12, no. 2, pp. 1124-1131

Pukrushpan, J.T., Peng, H.; & Stefanopoulou, A.G. (2004a). Control-oriented modeling and analysis for automotive fuel cell systems, *Transactions of the ASME*, vol. 126, no. 2, pp. 14-25

Pukrushpan, J.T.; Stefanopoulou, A.G. & Peng, H. (2004b). *Control of fuel cell power systems: principles, modeling, analysis, and feedback design*. New York: Springer- Verlag

Rapoport, I.; & Oshman, Y., (2007). Efficient fault tolerant estimation using the IMM methodology, IEEE Transactions on Aerospace and Electronic Systems, vol. 43, no. 2, pp. 492 - 508

Riascos, L.A.M.; Simoes, M.G.; & Miyagi, P.E. (2007). A Bayesian network fault diagnostic system for proton exchange membrane fuel cells. *Journal of Power Sources*, vol. 165, pp. 267-278

Takagi, T.; & Sugeno, M. (1985). Fuzzy identification of systems and its applications to modeling and control, *IEEE Transactions on System, Man, & Cyberne*tics vol. 15, no. 1, pp. 116–132

Tudoroiu, N.; & Khorasani, K. (2005). Fault detection and diagnosis for satellite's attitude control system using an interactive multiple model approach, *Proceedings of 2005 IEEE Conf. Control Applications*, pp. 28-31, Toronto, Ont.

Venkatasubramanian, V.; Rengaswamy, R.; Kavuri, S.N.; & Yin, K. (2003a). A review of process fault detection and diagnosis part III: process history based methods. *Computers and Chemical Engineering*, vol. 27, no. 3, pp. 327-346

Venkatasubramanian, V.; Rengaswamy, R.; Yin, K.; & Kavuri, S.N. (2003b). A review of process fault detection and diagnosis part I: quantitative model-based methods. *Computers and Chemical Engineering*, vol. 27, no. 3, pp. 293-311

Willsky, A. (1976). A survey of design methods for failure detection in dynamic systems. *Automatica*, vol. 12, pp. 601—611

Yen, G.G.; & Ho, L.W. (2003). Online multiple-model-based fault diagnosis and accommodation, *IEEE Transactions on Industrial Electronics*, vol. 50, no. 2, pp. 296 - 312

Zhang, Y.; & Jiang, J. (2001). Integrated active fault-tolerant control using IMM approach, *IEEE Transactions on Aerospace and Electronic Systems*, vol. 37, no. 4, pp. 1221 - 1235

Zhang, Y.; & Li, X.R. (1998). Detection and diagnosis of sensor and actuator failures using IMM estimator. *IEEE Transactions on Aerospace and Electronic Systems*, vol. 34, no. 4, pp. 1293—1311

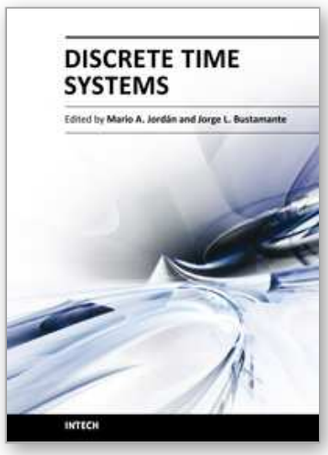

Discrete Time Systems

Edited by Dr. Mario Alberto JordÃ¡n

ISBN 978-953-307-200-5

Hard cover, 526 pages

Publisher InTech

Published online 26, April, 2011

Published in print edition April, 2011

Discrete-Time Systems comprehend an important and broad research field. The consolidation of digital-based computational means in the present, pushes a technological tool into the field with a tremendous impact in areas like Control, Signal Processing, Communications, System Modelling and related Applications. This book attempts to give a scope in the wide area of Discrete-Time Systems. Their contents are grouped conveniently in sections according to significant areas, namely Filtering, Fixed and Adaptive Control Systems, Stability Problems and Miscellaneous Applications. We think that the contribution of the book enlarges the field of the Discrete-Time Systems with signification in the present state-of-the-art. Despite the vertiginous advance in the field, we also believe that the topics described here allow us also to look through some main tendencies in the next years in the research area.

InTech Europe

University Campus STeP Ri
Slavka Krautzeka 83/A
51000 Rijeka, Croatia
Phone: +385 (51) 770 447
Fax: +385 (51) 686 166
www.intechopen.com

InTech China

Unit 405, Office Block, Hotel Equatorial Shanghai
No.65, Yan An Road (West), Shanghai, 200040, China
中国上海市延安西路65号上海国际贵都大饭店办公楼405单元
Phone: +86-21-62489820
Fax: +86-21-62489821

IntechOpen